



Published in final edited form as:

FASEB J. 2021 May ; 35(5): e21552. doi:10.1096/fj.202100027R.

Microbial-derived indoles inhibit neutrophil myeloperoxidase to diminish bystander tissue damage

Erica E. Alexeev^{1,2,*}, Alexander S. Dowdell^{1,*}, Morkos A. Henen^{3,4,*}, Jordi M. Lanis¹, J. Scott Lee¹, Ian M. Cartwright¹, Rachel E. M. Schaefer¹, Alfredo Ornelas¹, Joseph C. Onyiah¹, Beat Vögeli³, Sean P. Colgan^{1,†}

¹Mucosal Inflammation Program, Department of Medicine, University of Colorado Anschutz Medical Campus, Aurora, CO 80045, USA

²Inflammatory Bowel and Immunobiology Research Institute, Cedars-Sinai Medical Center, Los Angeles, CA 90048

³Department of Biochemistry and Molecular Genetics, University of Colorado Anschutz Medical Campus, Aurora, CO 80045, USA

⁴Department of Pharmaceutical Organic Chemistry, Mansoura University, Mansoura, 35516, Egypt.

Abstract

During episodes of acute inflammation, polymorphonuclear leukocytes (PMNs) are actively recruited to sites of inflammation or injury where they provide anti-microbial and wound-healing functions. One enzyme crucial for fulfilling these functions is myeloperoxidase (MPO), which generates hypochlorous acid from Cl⁻ and hydrogen peroxide. The potential exists, however, that uncontrolled extracellular generation of hypochlorous acid by MPO can cause bystander tissue damage and inhibit the healing response. Previous work suggests that the microbiota-derived tryptophan metabolites 1*H*-indole and related molecules (“indoles”) are protective during intestinal inflammation, although their precise mechanism of action is unclear. In the present work, we serendipitously discovered that indoles are potent and selective inhibitors of MPO. Using both primary human PMNs and recombinant human MPO in a cell-free system, we revealed that indoles inhibit MPO at physiologic concentrations. Particularly, indoles block the chlorinating activity of MPO, a reliable marker for MPO-associated tissue damage, as measured by coulometric-coupled HPLC. Further, we observed direct interaction between indoles and MPO using the established biochemical techniques microscale thermophoresis and STD-NMR. Utilizing a murine colitis model, we demonstrate that indoles inhibit bystander tissue damage, reflected in decreased colon 3-chlorotyrosine and pro-inflammatory chemokine expression *in vivo*. Taken together, these results identify microbiota-derived indoles acts as endogenous immunomodulatory

† Corresponding author: Sean P. Colgan, Ph.D., University of Colorado School of Medicine, 12700 East 19th Ave. MS B-146, Aurora, CO 80045, Office phone: 303-724-7235 Fax: 303-724-7243, Sean.Colgan@CUAnschutz.edu.

*These authors contributed equally to this work.

Author Contributions

E.E.A., A.S.D., M.A.H., B.V., and S.P.C. designed research. E.E.A., A.S.D., M.A.H., I.M.C., R.E.M.S., and B.V. performed research. E.E.A., A.S.D., M.A.H., J.M.L., J.S.L., I.M.C., R.E.M.S., J.C.O., B.V., and S.P.C. analyzed data and wrote paper.

Conflict of Interest

The authors state that no conflicts of interest exist in connection with this manuscript.

compounds through their actions on MPO, suggesting a symbiotic association between the gut microbiota and the host innate immune system. Such findings offer exciting new targets for future pharmacological intervention.

Introduction

Acute inflammatory responses are characterized by the recruitment of large numbers of polymorphonuclear leukocytes (PMNs) to sites of infection or injury. In the intestine, for example, the accumulation of PMNs within the mucosa stands in stark contrast with their paucity in healthy tissue, and consequently the enumeration of PMNs in the intestinal mucosa is one reliable metric for grading severity of disease by histology(1, 2). Following migration to the site of insult, PMNs transmigrate through the intestinal epithelium into the intestinal lumen, where they fulfill antimicrobial roles through a variety of mechanisms(3). One such mechanism involves the generation of hypochlorous acid (HOCl) from hydrogen peroxide (H_2O_2) by the enzyme myeloperoxidase (MPO), the most abundant PMN protein at 5% of the cell's dry weight(4–6). PMNs, upon ingestion of microbes via phagocytosis, undergo a “respiratory burst” in which NADPH oxidase generates superoxide ($O_2^{\cdot-}$) through the reduction of molecular oxygen (O_2)(7). Superoxide dismutase then catalyzes the disproportionation of $O_2^{\cdot-}$ to H_2O_2 . Within the phagosome, MPO utilizes H_2O_2 and free halide ions to generate hypohalous acids, with HOCl being the primary product due to MPO's utilization preference for chloride (Cl^-) anions(8). HOCl is a potent oxidizing agent and reacts indiscriminately with sulfur and nitrogen atoms, such as those found in the amine, amide, thiol, and thioester functional groups(9). Notably, HOCl reacts with aromatic groups such as the phenol moiety of tyrosine to generate chlorinated products – the modified amino acid 3-chlorotyrosine has been demonstrated to be a reliable marker of HOCl oxidation of tyrosine-containing proteins and a biomarker for MPO-mediated tissue damage(10–12). HOCl is a potent anti-bacterial agent, with efficacy in the sub-micromolar concentration and an estimated 1000-fold greater potency in the killing of *E. coli* than its precursor H_2O_2 (13, 14).

In addition to the release of MPO into phagocytic vesicles, PMNs also secrete MPO into the extracellular milieu through a process termed degranulation(15). Upon stimulation by a secretagogue such as IL-8, PMNs release specific granular proteins, including MPO, in a Ca^{2+} -dependent manner(15, 16). Notably, MPO itself has been shown to induce degranulation in PMNs, potentially resulting in further secretion of inflammatory mediators in a positive feedback loop(17, 18). Although PMNs play crucial roles in gut homeostasis, including defense against invasive microbes and maintenance of epithelial barrier function, uncontrolled PMN activity in the intestinal mucosa has been demonstrated to promote bystander damage of tissue and can delay or block resolution of inflammation(19–21). As such, PMNs have been described as “double-edged swords” due to their roles in both resolution and propagation of inflammation, and inhibition of their main mediator MPO has been consequently proposed as a means of limiting pathogenic PMN activity(22, 23). Recently, MPO activity has also been reported in PMN-derived extracellular vesicles, or microparticles, that have been demonstrated to inhibit wound healing in both *in vitro* and *in*

vivo models of tissue repair, further implicating MPO in pathogenic inhibition of the healing response (24).

One of the primary mechanisms by which the intestinal immune response is regulated is through the action of gut microbiota-derived metabolites(25). The human gut microbiota is composed of $>10^{13}$ individual microbes, at least as numerous as the cells in the host body and is primarily constituted of eubacteria, although other constituents (including archaea, fungi, protists, and viruses) are present but not as well characterized(26, 27). The gut microbiota generates various metabolites that have been previously assessed for their association with inflammatory bowel disease (IBD) – although hampered by various limitations in approaches, population heterogeneity, and the confounding influence of IBD treatment on the gut microbiota itself (e.g. intestinal resection), several classes of metabolites have been found to be significantly dysregulated in IBD patients(28).

Previously, we demonstrated that the microbiota-derived metabolite indole 3-propionate (IPA) is important in the regulation of intestinal epithelial homeostasis(29). IPA is produced exclusively from tryptophan metabolism by select species of the gut microbiota, and its concentration has been found to be reduced in patients with active IBD and in mice treated with colitogens(29–31). IPA has been shown to exert its effects through aryl hydrocarbon receptor (AhR)-mediated induction of the IL-10 receptor, although other pathways such as indole-mediated regulation of epithelial barrier function via the pregnane X receptor (PXR) have also been uncovered(29, 32). Mice treated with IPA in the dextran sodium sulfate (DSS) and indomethacin models of intestinal inflammation were protected from disease, as indicated by statistically significant changes in colitis-associated metrics such as colon shortening and weight loss, versus untreated counterparts(29, 32). Importantly, other gut microbiota-derived indoles have been shown to exert a positive influence in models of intestinal inflammation, suggesting that this class of molecules plays a crucial role in maintaining intestinal epithelial homeostasis(29, 32–34). Differential metabolism of tryptophan by “disease-associated” gut microbiota constituents vs “healthy-gut” associated members points towards a causative role for tryptophan derivatives, such as indoles, in the pathogenesis of inflammatory disorders (33). Likewise, indole metabolites have been implicated in regulation of intestinal barrier function and corresponding protection against liver inflammation (35). Indole derivatives generated from human milk oligosaccharides by *Bifidobacterium* species have further been shown to reduce inflammation and are hypothesized to be beneficial for the reduction of infant morbidity and mortality (36). Finally, previous reports suggest that indole may potentially inhibit the chlorinating activity of MPO; however, it is unclear whether this activity mediates the observed anti-inflammatory activity of indoles previously described in the context of acute intestinal inflammation (37).

In the present work, we provide evidence that indole metabolites specifically bind and inhibit PMN MPO activity. At physiologically relevant concentrations, indole and indole derivatives inhibit MPO activity in a competitive manner to reduce MPO-mediated tyrosine chlorination. Extensions of these studies reveal that delivery of IPA to mice with active colitis decreases inflammatory markers and specifically inhibits tissue tyrosine chlorination, a biomarker for *in vivo* tissue damage by MPO(10–12). Taken together, these results provide

a novel mechanism for microbial-derived indoles in the protection from bystander tissue damage mediated by PMN MPO.

Materials & Methods

Cell Culture and Reagents

T84 colorectal adenocarcinoma cells (ATCC# CCL-248) are a well-characterized *in vitro* model of the colonic intestinal epithelium and were grown as previously described(38–45). Briefly, cells were cultured at 37 °C, 5% CO₂ in 1:1 DMEM/F-12 (Thermo-Fisher# 11330–032) supplemented with heat-inactivated bovine calf serum (Hyclone# SH30072.03), GlutaMAX (Thermo-Fisher# 35050–061), and penicillin/streptomycin (Thermo-Fisher# 15140–122). Cells were passaged weekly using trypsin (Thermo-Fisher# 25200–056) dissociation and sub-cultured into 6-well plates. IPA, 1*H*-indole (CAS# 120–72-9, hereafter referred to as “indole”), and indole 3-acetic acid (IAA) were purchased from Sigma-Aldrich. The MPO inhibitor 4-aminobenzoic acid hydrazine (4-ABAH) was purchased from Cayman Chemical (Cat# 14845).

Animal Studies

C57BL/6 mice were bred and maintained on-site at the University of Colorado Anschutz vivarium. All protocols were approved by the University’s Institutional Animal Care and Use Committee (IACUC). Induction of colitis in mice with the colitogen DSS was performed as previously described(29, 38, 42, 45–47). Briefly, DSS (MW = 36,000–50,000, MP Biomedicals# 0216011080) was administered at 2.5% (w/v) in drinking water to mice (9–12 weeks old) for 9 days. IPA was given at 0.1 mg/mL in drinking water through the course of the experiment to one age- and sex-matched cohort. At the conclusion of the experiment, mice were euthanized by CO₂ asphyxiation + cervical dislocation and tissues collected. A portion of colon tissue was fixed in 10% neutral buffered formalin and stained using hematoxylin and eosin (H&E) for histopathological analysis. Stained colon sections were graded for PMN infiltration and crypt abscesses in a blinded manner. A second portion of colon was harvested into lysis buffer for further analysis of protein content by Olink proximity extension technology. In some instances, colon tissue was digested for analysis of tyrosine and chlorinated tyrosine by EC-HPLC (see below).

In vitro MPO Assay

Recombinant human MPO (rhMPO) was purchased from R&D Systems (Cat.# 3174-MP-250) and dissolved at 1 mg/mL using sterile ultrapure H₂O. Aliquots were then frozen at –80 °C and thawed individually as needed. For analysis of MPO activity in the presence of indoles, MPO was used at 1.67 µg/mL final concentration in a reaction buffer consisting of 133 mM sodium citrate, pH 4.2; 367 µg/mL 2,2’-Azino-bis(3-ethylbenzothiazoline-6-sulfonic acid) diammonium salt (ABTS, Sigma-Aldrich# A9941, dissolved fresh in ultrapure H₂O); and 6.53 mM H₂O₂ (Sigma-Aldrich# H1009, diluted fresh at time of experiment). Reactions were incubated 5min at room temperature, then quenched by addition of sodium dodecyl sulfate (SDS) to 0.5% (w/v). For competitive inhibition assays, the amount of initial ABTS was adjusted to the concentration given in the data figure and the background absorbance of samples without rhMPO subtracted from rhMPO-containing ones. For

determination of free-radical quenching by indole, the reactions were prepared as usual without indole, and indole was then added to the final concentration after the addition of SDS.

PMN Assays

Primary human PMNs were freshly isolated from healthy volunteers using gelatin or HistoPaque centrifugation as described in detail elsewhere (48). PMNs were resuspended in Hanks Balanced Salt Solution without divalent cations (HBSS⁻, Sigma-Aldrich# 4891, pH 7.4, made according to the manufacturer's instructions except that 10 mM HEPES was included). For quantification of effect of indole metabolites on PMN MPO activity, cells were incubated for 15 minutes at 4 °C with the indicated concentration of inhibitor in Hanks Balanced Salt Solution containing divalent cations (HBSS⁺) (Sigma-Aldrich# H1387, pH 7.4, prepared as directed by the manufacturer except that 10mM HEPES was included) and with Triton X-100 at a final concentration of ~0.5% (v/v). The resulting lysate was added directly to the reaction mixture used for rhMPO/ABTS assays described above with rhMPO omitted from the reaction. Reactions were incubated for 10 minutes, then stopped using SDS and the oxidation of ABTS measured by absorbance at 405nm. For measurement of MPO release from activated PMNs by ELISA, PMNs were incubated with 1 μM phorbol 12-myristate 13-acetate (PMA) and varying concentrations of indole for 15 minutes at 37 °C with gentle rotation. Afterwards, cells were gently spun and MPO quantified in the resulting supernatants using a commercial ELISA kit (Abcam# ab272101) according to the manufacturer's instructions.

Analysis of Gene Expression by Quantitative Real-Time Reverse Transcription PCR (qRT-PCR)

T84 cells were treated with HBSS⁺ with a final pH lowered to 6.0 using 12N HCl. HBSS⁺ pH 6.0 included H₂O₂ at 163 μM and rhMPO at 1.67 μg/mL. Indole was included in some samples at 0.833 mM final concentration. Cells were incubated for 30 minutes at 37 °C, 5% CO₂ with rhMPO reaction mixture, then washed with PBS and incubated for a further 4hr in growth media. After this time, cells were collected in cold TRIzol reagent (Thermo-Fisher# 15596-026), and lysates stored at -80 °C. Total RNA was purified from TRIzol lysates according to the manufacturer's instructions. cDNA was synthesized from total RNA using iScript cDNA Supermix (Bio-Rad# 1708841), then analyzed on an Applied Biosystems 7300 real-time PCR instrument using Power SYBR Green PCR Master Mix (Thermo-Fisher# 4367659). Primers used for qRT-PCR are given in Table 1 and were ordered from Thermo-Fisher using sequences from Harvard PrimerBank (49).

Analysis of Inflammatory Markers using Olink

Proteins from colitic tissues (DSS±IPA) were measured with the Olink panel using proximity extension amplification (PEA) technology, a high-throughput multiplex proteomic immunoassay(50). The assay uses epitope-specific binding and hybridization of a set of paired oligonucleotide antibody probes, which is subsequently amplified using a quantitative PCR, resulting in log base-2 normalized protein expression (NPX) values.

Analysis of MPO Chlorination Activity by EC-HPLC

Tyrosine (Tyr) conversion to 3-chlorotyrosine (3-Cl-Tyr) by rhMPO was performed by incubating rhMPO (stock 250 $\mu\text{g/ml}$) with Tyr (200 μM) and H_2O_2 (200 μM) in a solution containing 100 mM NaCl with or without indicated concentrations of indole or IPA. Reactions were allowed to proceed for 1hr at 37 °C and stopped by addition of excess methionine (2 mM).

Tyr and 3-Cl-Tyr were quantified using isocratic reversed-phase high-performance liquid chromatography with electrochemical coulometric array detection (EC-HPLC)(Coularray, Thermo Scientific, Waltham, MA). Separation was achieved using an Acclaim Polar Advantage II C18 column, 5 μm 120Å, 4.6 \times 150 mm, (Thermo-Fisher) at a flow rate of 0.6 mL/min in a mobile phase consisting of 10% acetonitrile in 50 mM sodium phosphate buffer, pH 3, containing 0.42 mM octanesulphonic acid as an ion-pairing agent. The data were collected and quantified using the Coularray software with comparison to Tyr (Sigma-Aldrich) and 3-Cl-Tyr (Alfa Aesar, Ward Hill, MA) standards. For analysis of MPO chlorination *in vivo*, colon tissue from mice treated with DSS and either with/without IPA was sonicated and digested overnight at 37 °C using 5 mg/mL Pronase (1mg/ml, Sigma-Aldrich# 10165921001). The digests were then spun to pellet insoluble material, and the resulting supernatants were filtered through 5 kDa molecular weight cutoff spin columns (Sartorius# VS0112) prior to HPLC analysis.

Nuclear Magnetic Resonance Spectroscopy (NMR) of rhMPO/Indoles

To study ligand binding, saturation transfer difference (STD) NMR experiments were conducted(51). In STD, a frequency selective train of pulses is applied at a protein resonance in a region outside the spectral region of the ligand. This results in efficient saturation of the protein spins via spin diffusion. In case of presence of ligand spins in proximity of the protein, the saturation is transferred to the ligand resulting in reduction of the NMR signal intensity. The experiment is performed once with the saturation pulses applied off-resonance (control), and then repeated with the saturation pulses applied on-resonance. Upon subtraction of the saturated from the reference spectrum, there will be peaks if binding occurs in the medium to weak range, while peaks cancel out in case of lack of binding or tight binding. The experiments were carried out on a 600 MHz triple-resonance Varian cryoprobe spectrometer at 25 °C. 1D ^1H spectra were recorded with 16,384 complex points, 512 scans, and an interscan delay of 1.5s. Selective saturation was achieved using a cascade of Gaussian pulses with lengths of 50 ms during a total time of 3 s. On-resonance saturation was applied at -0.5 ppm and off-resonance saturation at 20 ppm. To eliminate background protein resonances from the spectrum, a spin-lock filter ($\text{T}1\rho$ -filter) was used for 30 ms. All spectra were processed using NMRPipe and analyzed with NMRDraw(52). The concentrations of the tested ligands and the protein were 1 mM and 9 μM , respectively. Protein and tested ligands were all dissolved in PBS, pH 6.0.

Microscale thermophoresis (MST) Experiments:

Measurements were carried out on a NanoTemper Monolith NT.115 pico instrument (NanoTemper Technologies) at 25°C using medium power and 20% excitation power (auto-detect-pico-red). MPO::6xHis was fluorescently labeled by interacting 100 μL protein

solution (200 nM concentration) with 100 μ L Red-Tris NTA dye (100 nM concentration). The reaction mixture was incubated at room temperature for 30 min followed by centrifugation for 10 min at 4°C with 15,000 $\times g$. Then, between 5–50 nM of labeled MPO::6xHis and 16 two-fold dilution series of the tested ligands were loaded into 16 standard capillaries (NanoTemper Technologies) (highest concentrations of indole, indole-3-propionic acid, and 4-ABAH: 5 mM, 1.25 mM, and 5 mM). We observed sigmoidal behavior of the fluorescence level over time, which allowed characterization of the interactions. Raw data were analyzed using the NanoTemper software (MO affinity analysis v2.2.7). The signal-to-noise ratios for indole, indole-3-propionic acid, and 4-ABAH were 12.9, 10.5, and 24.2, respectively.

Results

Indole Metabolites Inhibit MPO Activity *In vitro*

Based on our previous analysis of indole metabolites in inflammatory models (29), we examined the influence of indoles on PMN transmigration *in vitro*. Serendipitously, we observed that our endpoint for PMN transmigration (MPO) was diminished by the presence of indole and indole metabolites. The observation suggested that indoles inhibit the chlorinating activity of MPO. Upon further examination, such inhibition of MPO activity by indoles is consistent with a previous report suggesting that indole-containing molecules inhibit the chlorinating activity of MPO(37).

To examine mechanisms of MPO inhibition by indoles, we expanded our analysis using primary human PMNs. Incubation of PMN lysates with IPA, indole, or IAA (each at 1 mM) resulted in significant inhibition of peroxidase activity, as measured by ABTS oxidation at $\lambda = 405\text{nm}$ (Figure 1A). Indole was also found to inhibit PMN-derived MPO in a dose-dependent manner, although it was not as efficient as the commercial inhibitor 4-ABAH under our *in vitro* reaction conditions (Supplemental Figure 1A). Although we utilized cellular lysates in these analyses, indoles have been previously shown to freely diffuse across lipid membranes; therefore, it would be expected that indoles could similarly inhibit intracellular MPO (i.e. in the phagosome) with corresponding effects on post-phagocytosis phenomena, a theory actively under exploration by our group (53, 54). We also asked whether indole could affect the *in vitro* secretion of MPO (degranulation) from activated PMNs. To answer this, primary human PMNs were activated with 1 μ M PMA and with varying concentrations of indole, and MPO in the resulting supernatants was quantified using a commercial ELISA kit (55). We observed that the inclusion of indole during PMN activation had no influence on the quantity of extracellular MPO, suggesting that indole does not impact degranulation of activated PMNs (Supplemental Figure 1B).

As MPO is the most abundant protein (and therefore peroxidase) in PMNs, we surmised that these metabolites were inhibiting MPO(6). However, the possibility existed that IPA, indole, and IAA could also inhibit other components necessary for MPO activity in PMNs, such as NADPH oxidase. To answer this question, we measured the activity of rhMPO in a minimal, cell-free system using H_2O_2 and varying concentrations of IPA, indole, or IAA. We found that these indole metabolites inhibited rhMPO in a dose-dependent manner (Figure 1B), indicating that the previously observed inhibition of whole-cell PMN MPO was due to direct

action of indole metabolites on MPO itself rather than any secondary action and recapitulating our earlier results showing dose-dependent inhibition of MPO by indole in PMNs. In addition, we found that the inhibition of MPO by indole occurred competitively, as increasing the initial concentration of ABTS allowed for the inhibition of indole to be overcome (Supplemental Figure 2A). Increasing the initial concentration of the other substrate, H₂O₂, was found to be detrimental to rhMPO activity, presumably from loss of enzyme activity due to oxidative stress or protein denaturation(56, 57). As free radical scavengers have been shown to eliminate ABTS absorbance at 405nm, and because indoles have been previously described as antioxidants, we asked whether our observed inhibition of MPO by indoles was due to quenching of the ABTS radical cation(58, 59). Addition of indole to a complete cell-free rhMPO reaction showed no change in absorbance at 405nm (Supplemental Figure 2B), indicating that the amount of ABTS radical cation remained unchanged by indole and the previously observed inhibition of MPO by indole metabolites was likely due to an influence on the enzyme itself.

Finally, we asked whether inhibition of MPO activity by indole could diminish pro-inflammatory signaling *in vitro*. For this, we exposed T84 intestinal epithelial cells with rhMPO +/- indole and assessed pro-inflammatory gene expression by qRT-PCR. Our hypothesis was that, even in the absence of immune cells and gut microbiota, indole metabolites could singularly reduce MPO-mediated induction of inflammation. We found that expression of the potent PMN chemoattractant IL-8 (CXCL8) was significantly reduced by inclusion of indole at a physiological concentration (0.833 mM) (Figure 1C), indicating that the inhibition of MPO by indole could prevent pro-inflammatory stimulus in a minimal, *in vitro* system. These results suggest that indoles regulate PMN activity, and thereby modulate inflammatory stimulus, through inhibition of MPO.

Indoles Inhibit Tyrosine Chlorination by MPO

We further sought to clarify the ability of indoles to inhibit the activity of MPO *in vitro*, as some reports have described the ability of indoles to quench ABTS absorbance in an enzyme-free system(60). To do so, we adapted our previous cell-free rhMPO assay for the measurement of tyrosine chlorination. As mentioned in the *Introduction*, MPO-derived HOCl reacts with the phenol moiety of tyrosine to generate 3-chlorotyrosine, and this chlorinated amino acid has been demonstrated to be a reliable biomarker of PMN-mediated tissue damage *in vivo*(10–12). As such, a reduction in tyrosine chlorination by indoles would suggest a protective mechanism during acute intestinal inflammation. As shown in Figure 2A, tyrosine and 3-chlorotyrosine were distinctly detectable by HPLC coupled to electrochemical coulometric detection. Utilizing this established method, rhMPO was reacted with H₂O₂, free tyrosine, and, as appropriate, various concentrations of indole and indole 3-propionic acid. Indole and IPA both inhibited chlorination of free tyrosine in a dose-dependent manner (Figure 2B), with the highest indole/IPA doses tested (1 mM) completely abolishing tyrosine chlorination. This complete inhibition is noteworthy as indole has been reported at millimolar concentrations in healthy adults and suggests a robust mechanism for regulation of PMN chlorinating activity(61, 62).

Characterization of the Interaction between Indoles and MPO via STD-NMR and MST

We next sought to determine the nature by which indoles and MPO interact. As a starting point, we defined whether indole and MPO directly interact using microscale thermophoresis analysis (MST). In MST, the binding of a nonfluorescent ligand to a fluorescent protein is measured through the induction of temperature gradients(63). Using a fluorescently labeled MPO, we compared the binding affinity of indole and the MPO inhibitor 4-ABAH by MST. As shown in Figure 3, we found that both indole and 4-ABAH show saturable binding and possess affinities of $272.0 \pm 77.4 \mu\text{M}$, and $409.0 \pm 66.7 \mu\text{M}$, respectively. Interestingly, we observed indole to possess a stronger binding affinity to MPO than the commercially available inhibitor 4-ABAH. The reason for the discrepancy between the observed higher affinity of indole for MPO versus 4-ABAH by MST, despite the increased efficacy of 4-ABAH in our cell-based assays, is unclear but could stem from the nuances of the *in vitro* assays used to examine MPO/inhibitor interactions in this work.

We extended these results to examine direct binding of indole and MPO. To accomplish this, we examined the interaction between rhMPO (9 μM) and either indole, IPA, or tryptophan (1 mM) using ligand-based Saturation Transfer Difference NMR (STD-NMR). The resulting STD-NMR plots are shown in Figure 4 and reflect the difference in ^1H -NMR signal between the ligand reference spectrum and the ligand spectrum following MPO-transferred saturation(64, 65). As shown in Figures 4A and 4B, indole and IPA, respectively, both demonstrate binding to rhMPO under the conditions used as indicated by the peaks in the NMR plots. In contrast, their precursor tryptophan does not demonstrate appreciable binding to rhMPO by STD-NMR (Figure 4C). As IPA and tryptophan differ only by the presence of an amine group on the α -carbon, this suggests that the amine group in tryptophan prevents association with MPO. Finally, as a control the known MPO inhibitor, 4-ABAH(66, 67), was tested for binding to MPO by STD-NMR. Although it demonstrated no STD signature (Figure 4D), this was most likely due to its strong, irreversible inhibition of MPO ($\text{IC}_{50} = 0.3 \mu\text{M}$) and would account for the potent inhibition of PMN-derived MPO described above. As STD-NMR relies on the measurement of the signal of bulk free ligand after the release of the bound ligand following saturation transfer, a very strongly bound ligand would produce a similar STD-NMR plot to one that does not bind at all. Taken together, these results demonstrate that indole binds MPO in a specific manner to inhibit MPO enzymatic activity.

Influence of IPA on tissue damage in murine colitis

The infiltration of PMNs is a hallmark of intestinal inflammation and is well-documented in both murine models of colitis and in biopsies from human UC and CD patients(3). Infiltrating PMNs secrete various pro-inflammatory factors including MPO which, in turn, generates the potent oxidant HOCl – a potential source of bystander tissue damage. Previously, our group observed amelioration of intestinal inflammation and protection against colitic disease in mice administered the gut microbiota-derived metabolite IPA(29). To assess the role of IPA in regulating MPO-mediated bystander tissue damage, we exposed mice to either vehicle (water) or IPA (0.1 mg/ml) *ad libitum* during the course of DSS colitis and collected colon tissue for histologic, biochemical and RNA analyses. As shown in Figure 5A, DSS-induced colitis resulted in the formation of significant tissue damage, including the formation of large crypt abscesses. To examine the impact IPA on MPO-

mediated tissue damage, we quantified the levels of 3-Cl-Tyr in whole mouse colon tissue following acute DSS colitis either with or without IPA intervention. Administration of IPA significantly reduced colonic 3-Cl-Tyr (Figure 5B), demonstrating that the inhibition of MPO activity by indole/IPA correlates with the protective effect of IPA *in vivo*. Further analysis of pro-inflammatory markers in murine colonic tissue using Olink PEA technology revealed that the chemokines Cxcl1, Ccl3, and Ccl5 were decreased in DSS/IPA-treated mice compared to their DSS-only counterparts (Figure 5C). These data indicate that IPA functions to diminish PMN MPO-mediated tissue damage during intestinal inflammation *in vivo*.

Discussion

PMNs function as a “first line of defense” against pathogens and are the vanguard of immune cells recruited to nascent sites of inflammation(68). PMNs have also recently been found to be indispensable for wound healing and re-vascularization following injury, suggesting additional roles beyond elimination of pathogens(69, 70). However, dysregulated PMN activity can be destructive to healthy tissue and can result in a feedback loop of uncontrolled inflammation(21, 23). This is especially evident in IBD, where PMN infiltration is a histopathological hallmark of active disease(21, 71, 72). A significant feature of active IBD is dysbiosis of the gut microbiota, with an accompanying shift in microbiota-derived metabolites(73–75). Gut microbiota metabolites have been previously demonstrated to regulate the immune response, both locally in the gastrointestinal tract and systemically(76, 77). Of these metabolites, tryptophan derivatives, such as the indole and indole derivatives, have attracted significant attention for their ability to regulate multiple aspects of both innate and adaptive immunity(29, 78–81). Importantly, indole metabolites have been observed to be dysregulated in patients with active IBD and in mouse models of colitis, and restoration of depleted indoles in animal models of IBD reduce disease severity(29). These observations suggest that indole metabolites might be used both as a biomarker for disease and as a therapeutic.

In the present work, we demonstrate that MPO, both derived from primary human PMNs and recombinant enzyme, is inhibited by indoles at physiologic concentrations. This inhibition blocks generation of the oxidant HOCl and chlorination of tyrosine residues both *in vitro* and *in vivo*, and the effect of indole appears to be independent of PMN degranulation. As 3-chlorotyrosine is a biomarker that is indicative of PMN-associated tissue damage, this inhibition suggests a mechanism for the protective influence observed by histological examination of IPA-treated mice subjected to the colitogen DSS(10–12). This is supported by findings that indoles reduce expression of pro-inflammatory chemokines both *in vitro* and *in vivo*. Within this study, we further demonstrate that indoles bind to recombinant MPO, an observation reinforced by *in vitro* data showing that MPO inhibition by indoles is due to competitive inhibition. Such observations are consistent with previous work(37) showing that various indole ring substituted molecules inhibit the chlorinating activity of MPO. It is notable that the peroxidation activity of MPO proceeds through redox intermediates, termed MPO-I and MPO-II, where only MPO-I can oxidize chloride ion. Using spectral scanning, Ximenes *et al.* demonstrated that MPO inhibition by indole occurred through the accumulation of the redox intermediate MPO-II, which lacks

chlorinating activity. Taken together, the data presented herein provide a compelling argument for the mechanism by which indoles modulate PMN activity, and thereby acute inflammation, through regulation of the principle PMN inflammatory protein MPO. One possibility that cannot be excluded is the nonspecific interaction of cationic MPO and indole, which shows an effective negative charge at acidic pH values (82, 83). Given the specific binding of indole to MPO indicated by NMR and MST, we hypothesize that nonspecific electrostatic interactions do not fully account for the observed interaction; however, an increase in binding affinity promoted by electrostatic interactions remains a distinct possibility that should be explored further in future investigations.

The suppression of pro-inflammatory chemokines by indole metabolites in the *in vivo* DSS model of IBD suggests that indoles help alleviate the previously described positive feedback loop of inflammation mediated in part by MPO through bystander tissue damage (17, 18, 21, 23). Given that unregulated MPO activity in the context of acute intestinal inflammation is a driving force for expression of pro-inflammatory cytokines and chemokines, it is logical that inhibition of MPO by indoles can indirectly suppress their induction through reduction of inflammatory stimuli. To this extent, MPO inhibitors have been commercially developed and have been shown to be beneficial in the treatment of extraintestinal inflammatory disorders, including pulmonary, endothelial, and neurological inflammatory diseases (84–86). Although the potential direct effect of indoles on pro-inflammatory gene expression cannot be discounted, as demonstrated by the cell permeable nature of indoles and their previously shown ability to influence mammalian transcription, we surmise that the direct inhibition of MPO by indoles is a major contributing factor to the decrease in pro-inflammatory chemokine expression and interruption of the MPO-driven inflammatory positive feedback loop through ameliorating bystander tissue damage (53, 54, 78).

The endogenous nature of indole metabolites and their ability to regulate MPO in a dose-dependent manner may be evidence of co-evolution between gut bacteria and the host immune system. Selection pressure would result in the maintenance of mechanisms for avoiding an inappropriate immune response, such as the secretion of anti-inflammatory metabolites. This can be seen in the ability of other microbiota metabolites, such as SCFAs and polyamines, to exert anti-inflammatory influences on both the mucosa and immune cells (76, 87, 88). Given the ubiquity of indoles in the gut environment and their role in maintaining intestinal homeostasis, it would not be off base to surmise that the human GI tract has adapted to “require” these metabolites at certain concentrations for intestinal homeostasis. Indeed, the presence of microbial metabolites in other fluids, such as serum and cerebrospinal fluid, suggest that these metabolites may in fact regulate multiple bodily systems beyond the GI tract (89). IPA specifically has been previously assessed for its roles in ameliorating neurodegenerative disorders (such as Alzheimer’s Disease) and chronic kidney disease (90–93). Similarly, IAA has been linked to the reduction of inflammation in hepatocytes and macrophages, as well as prevention of nonalcoholic fatty liver disease (94, 95). These observations suggest that diseases other than IBD may in fact be dependent on gut microbiota-derived metabolites, a concept supported by correlative studies that identify co-morbidity between IBD and extra-intestinal inflammatory disorders such as asthma and rheumatoid arthritis (96, 97). Future studies might consider the hypothesis that manipulation

of the gut microbiota and/or its metabolites may be a unified means of addressing varied inflammatory disorders(98, 99).

In summary, we have identified indole metabolites as a class of anti-inflammatory compounds through their regulation of the PMN protein MPO and demonstrated *in vitro* and *in vivo* that indoles at physiologic concentrations modulate MPO activity to prevent inflammation and diminish PMN-mediated bystander damage. From this perspective, indole and its metabolites appear to be promising candidates as selective and reversible inhibitors of MPO.

Supplementary Material

Refer to Web version on PubMed Central for supplementary material.

Acknowledgements

This work was supported by NIH grants DK1047893, DK50189, DK095491, DK103639 and VA Merit BX002182. The authors would like to thank Rachael E. Kostecky for experimental assistance with PMN isolation.

List of Nonstandard Abbreviations

3-Cl-Tyr	3-chlorotyrosine
4-ABAH	4-aminobenzoic acid hydrazine
ABTS	2,2'-Azino-bis(3-ethylbenzothiazoline-6-sulfonic acid) diammonium salt
DSS	Dextran Sodium Sulfate
EC-HPLC	Electrochemical Coulometric array detection coupled High Performance Liquid Chromatography
IAA	Indole-3-acetic acid
IPA	Indole-3-propionic acid
MPO	Myeloperoxidase
MST	Microscale Thermophoresis
PMA	phorbol 12-myristate 13-acetate
PMN	Polymorphonuclear leukocyte
rhMPO	recombinant human MPO
STD-NMR	Saturation Transfer Difference Nuclear Magnetic Resonance Spectroscopy

References

1. DeRoche TC, Xiao SY, and Liu X (2014) Histological evaluation in ulcerative colitis. *Gastroenterol Rep (Oxf)* 2, 178–192 [PubMed: 24942757]
2. Villanacci V, Antonelli E, Geboes K, Casella G, and Bassotti G (2013) Histological healing in inflammatory bowel disease: a still unfulfilled promise. *World J Gastroenterol* 19, 968–978 [PubMed: 23467585]
3. Fournier BM, and Parkos CA (2012) The role of neutrophils during intestinal inflammation. *Mucosal Immunol* 5, 354–366 [PubMed: 22491176]
4. Schultz J, and Kaminker K (1962) Myeloperoxidase of the leucocyte of normal human blood. I. Content and localization. *Arch Biochem Biophys* 96, 465–467 [PubMed: 13909511]
5. Winterbourn CC (2002) Biological reactivity and biomarkers of the neutrophil oxidant, hypochlorous acid. *Toxicology* 181–182, 223–227
6. Heinecke JW, and Goldberg IJ (2014) Myeloperoxidase: a therapeutic target for preventing insulin resistance and the metabolic sequelae of obesity? *Diabetes* 63, 4001–4003 [PubMed: 25414015]
7. Chen Y, and Junger WG (2012) Measurement of oxidative burst in neutrophils. *Methods Mol Biol* 844, 115–124 [PubMed: 22262438]
8. Strzepa A, Pritchard KA, and Dittel BN (2017) Myeloperoxidase: A new player in autoimmunity. *Cell Immunol* 317, 1–8 [PubMed: 28511921]
9. Davies MJ (2011) Myeloperoxidase-derived oxidation: mechanisms of biological damage and its prevention. *J Clin Biochem Nutr* 48, 8–19 [PubMed: 21297906]
10. Kettle AJ (1996) Neutrophils convert tyrosyl residues in albumin to chlorotyrosine. *FEBS Lett* 379, 103–106 [PubMed: 8566218]
11. Fu S, Wang H, Davies M, and Dean R (2000) Reactions of hypochlorous acid with tyrosine and peptidyl-tyrosyl residues give dichlorinated and aldehydic products in addition to 3-chlorotyrosine. *J Biol Chem* 275, 10851–10858 [PubMed: 10753880]
12. Buss IH, Senthilmohan R, Darlow BA, Mogridge N, Kettle AJ, and Winterbourn CC (2003) 3-Chlorotyrosine as a marker of protein damage by myeloperoxidase in tracheal aspirates from preterm infants: association with adverse respiratory outcome. *Pediatr Res* 53, 455–462 [PubMed: 12595594]
13. Thomas EL (1979) Myeloperoxidase-hydrogen peroxide-chloride antimicrobial system: effect of exogenous amines on antibacterial action against *Escherichia coli*. *Infect Immun* 25, 110–116 [PubMed: 39030]
14. Lymar SV, and Hurst JK (1995) Role of compartmentation in promoting toxicity of leukocyte-generated strong oxidants. *Chem Res Toxicol* 8, 833–840 [PubMed: 7492732]
15. Lacy P (2006) Mechanisms of degranulation in neutrophils. *Allergy Asthma Clin Immunol* 2, 98–108 [PubMed: 20525154]
16. Meddows-Taylor S, Martin DJ, and Tiemessen CT (1999) Impaired interleukin-8-induced degranulation of polymorphonuclear neutrophils from human immunodeficiency virus type 1-infected individuals. *Clin Diagn Lab Immunol* 6, 345–351 [PubMed: 10225834]
17. Grigorieva DV, Gorudko IV, Sokolov AV, Kostevich VA, Vasilyev VB, Cherenkevich SN, and Panasencko OM (2016) Myeloperoxidase Stimulates Neutrophil Degranulation. *Bull Exp Biol Med* 161, 495–500 [PubMed: 27597056]
18. Lau D, Mollnau H, Eiserich JP, Freeman BA, Daiber A, Gehling UM, Brummer J, Rudolph V, Munzel T, Heitzer T, Meinertz T, and Baldus S (2005) Myeloperoxidase mediates neutrophil activation by association with CD11b/CD18 integrins. *Proc Natl Acad Sci U S A* 102, 431–436 [PubMed: 15625114]
19. Zindl CL, Lai JF, Lee YK, Maynard CL, Harbour SN, Ouyang W, Chaplin DD, and Weaver CT (2013) IL-22-producing neutrophils contribute to antimicrobial defense and restitution of colonic epithelial integrity during colitis. *Proc Natl Acad Sci U S A* 110, 12768–12773 [PubMed: 23781104]
20. Barry R, Ruano-Gallego D, Radhakrishnan ST, Lovell S, Yu L, Kotik O, Glegola-Madejska I, Tate EW, Choudhary JS, Williams HRT, and Frankel G (2020) Faecal neutrophil elastase-antiprotease balance reflects colitis severity. *Mucosal Immunol* 13, 322–333 [PubMed: 31772324]

21. Elliott SN, and Wallace JL (1998) Neutrophil-mediated gastrointestinal injury. *Can J Gastroenterol* 12, 559–568 [PubMed: 9926266]
22. Chami B, Martin NJJ, Dennis JM, and Witting PK (2018) Myeloperoxidase in the inflamed colon: A novel target for treating inflammatory bowel disease. *Arch Biochem Biophys* 645, 61–71 [PubMed: 29548776]
23. Williams IR, and Parkos CA (2007) Colonic neutrophils in inflammatory bowel disease: double-edged swords of the innate immune system with protective and destructive capacity. *Gastroenterology* 133, 2049–2052 [PubMed: 18054577]
24. Slater TW, Finkielstein A, Mascarenhas LA, Mehl LC, Butin-Israeli V, and Sumagin R (2017) Neutrophil Microparticles Deliver Active Myeloperoxidase to Injured Mucosa To Inhibit Epithelial Wound Healing. *J Immunol* 198, 2886–2897 [PubMed: 28242649]
25. Belkaid Y, and Hand TW (2014) Role of the microbiota in immunity and inflammation. *Cell* 157, 121–141 [PubMed: 24679531]
26. Sender R, Fuchs S, and Milo R (2016) Revised Estimates for the Number of Human and Bacteria Cells in the Body. *PLoS Biol* 14, e1002533 [PubMed: 27541692]
27. Matijasic M, Mestrovic T, Paljetak HC, Peric M, Baresic A, and Verbanac D (2020) Gut Microbiota beyond Bacteria-Mycobiome, Virome, Archaeome, and Eukaryotic Parasites in IBD. *Int J Mol Sci* 21
28. Lavelle A, and Sokol H (2020) Gut microbiota-derived metabolites as key actors in inflammatory bowel disease. *Nat Rev Gastroenterol Hepatol* 17, 223–237 [PubMed: 32076145]
29. Alexeev EE, Lanis JM, Kao DJ, Campbell EL, Kelly CJ, Battista KD, Gerich ME, Jenkins BR, Walk ST, Kominsky DJ, and Colgan SP (2018) Microbiota-Derived Indole Metabolites Promote Human and Murine Intestinal Homeostasis through Regulation of Interleukin-10 Receptor. *Am J Pathol* 188, 1183–1194 [PubMed: 29454749]
30. Dodd D, Spitzer MH, Van Treuren W, Merrill BD, Hryckowian AJ, Higginbottom SK, Le A, Cowan TM, Nolan GP, Fischbach MA, and Sonnenburg JL (2017) A gut bacterial pathway metabolizes aromatic amino acids into nine circulating metabolites. *Nature* 551, 648–652 [PubMed: 29168502]
31. Wikoff WR, Anfora AT, Liu J, Schultz PG, Lesley SA, Peters EC, and Siuzdak G (2009) Metabolomics analysis reveals large effects of gut microflora on mammalian blood metabolites. *Proc Natl Acad Sci U S A* 106, 3698–3703 [PubMed: 19234110]
32. Venkatesh M, Mukherjee S, Wang H, Li H, Sun K, Benechet AP, Qiu Z, Maher L, Redinbo MR, Phillips RS, Fleet JC, Kortagere S, Mukherjee P, Fasano A, Le Ven J, Nicholson JK, Dumas ME, Khanna KM, and Mani S (2014) Symbiotic bacterial metabolites regulate gastrointestinal barrier function via the xenobiotic sensor PXR and Toll-like receptor 4. *Immunity* 41, 296–310 [PubMed: 25065623]
33. Kaur H, Bose C, and Mande SS (2019) Tryptophan Metabolism by Gut Microbiome and Gut-Brain-Axis: An in silico Analysis. *Front Neurosci* 13, 1365 [PubMed: 31920519]
34. Hendriks T, and Schnabl B (2019) Indoles: metabolites produced by intestinal bacteria capable of controlling liver disease manifestation. *J Intern Med* 286, 32–40 [PubMed: 30873652]
35. Zhao ZH, Xin FZ, Xue Y, Hu Z, Han Y, Ma F, Zhou D, Liu XL, Cui A, Liu Z, Liu Y, Gao J, Pan Q, Li Y, and Fan JG (2019) Indole-3-propionic acid inhibits gut dysbiosis and endotoxin leakage to attenuate steatohepatitis in rats. *Exp Mol Med* 51, 1–14
36. Ehrlich AM, Pacheco AR, Henrick BM, Taft D, Xu G, Huda MN, Mishchuk D, Goodson ML, Slupsky C, Barile D, Lebrilla CB, Stephensen CB, Mills DA, and Raybould HE (2020) Indole-3-lactic acid associated with Bifidobacterium-dominated microbiota significantly decreases inflammation in intestinal epithelial cells. *BMC Microbiol* 20, 357 [PubMed: 33225894]
37. Ximenes VF, Paino IM, Faria-Oliveira OM, Fonseca LM, and Brunetti IL (2005) Indole ring oxidation by activated leukocytes prevents the production of hypochlorous acid. *Braz J Med Biol Res* 38, 1575–1583 [PubMed: 16258625]
38. Wang RX, Lee JS, Campbell EL, and Colgan SP (2020) Microbiota-derived butyrate dynamically regulates intestinal homeostasis through regulation of actin-associated protein synaptopodin. *Proc Natl Acad Sci U S A* 117, 11648–11657 [PubMed: 32398370]

39. Zheng L, Kelly CJ, Battista KD, Schaefer R, Lanis JM, Alexeev EE, Wang RX, Onyiah JC, Kominsky DJ, and Colgan SP (2017) Microbial-Derived Butyrate Promotes Epithelial Barrier Function through IL-10 Receptor-Dependent Repression of Claudin-2. *J Immunol* 199, 2976–2984 [PubMed: 28893958]
40. Kelly CJ, Zheng L, Campbell EL, Saeedi B, Scholz CC, Bayless AJ, Wilson KE, Glover LE, Kominsky DJ, Magnuson A, Weir TL, Ehrentraut SF, Pickel C, Kuhn KA, Lanis JM, Nguyen V, Taylor CT, and Colgan SP (2015) Crosstalk between Microbiota-Derived Short-Chain Fatty Acids and Intestinal Epithelial HIF Augments Tissue Barrier Function. *Cell Host Microbe* 17, 662–671 [PubMed: 25865369]
41. Dowdell AS, Cartwright IM, Goldberg MS, Kostecky R, Ross T, Welch N, Glover LE, and Colgan SP (2020) The HIF target ATG9A is essential for epithelial barrier function and tight junction biogenesis. *Mol Biol Cell* 31, 2249–2258 [PubMed: 32726170]
42. Cartwright IM, Curtis VF, Lanis JM, Alexeev EE, Welch N, Goldberg MS, Schaefer REM, Gao RY, Chun C, Fennimore B, Onyiah JC, Gerich ME, Dempsey PJ, and Colgan SP (2020) Adaptation to inflammatory acidity through neutrophil-derived adenosine regulation of SLC26A3. *Mucosal Immunol* 13, 230–244 [PubMed: 31792360]
43. Curtis VF, Cartwright IM, Lee JS, Wang RX, Kao DJ, Lanis JM, Burney KM, Welch N, Hall CHT, Goldberg MS, Campbell EL, and Colgan SP (2018) Neutrophils as sources of dinucleotide polyphosphates and metabolism by epithelial ENPP1 to influence barrier function via adenosine signaling. *Mol Biol Cell* 29, 2687–2699 [PubMed: 30188771]
44. Onyiah JC, Schaefer REM, and Colgan SP (2018) A Central Role for Heme Oxygenase-1 in the Control of Intestinal Epithelial Chemokine Expression. *J Innate Immun* 10, 228–238 [PubMed: 29791903]
45. Lee JS, Wang RX, Alexeev EE, Lanis JM, Battista KD, Glover LE, and Colgan SP (2018) Hypoxanthine is a checkpoint stress metabolite in colonic epithelial energy modulation and barrier function. *J Biol Chem* 293, 6039–6051 [PubMed: 29487135]
46. Gao RY, Shearn CT, Orlicky DJ, Battista KD, Alexeev EE, Cartwright IM, Lanis JM, Kostecky RE, Ju C, Colgan SP, and Fennimore BP (2020) Bile acids modulate colonic MAdCAM-1 expression in a murine model of combined cholestasis and colitis. *Mucosal Immunol*
47. Aherne CM, Saeedi B, Collins CB, Masterson JC, McNamee EN, Perrenoud L, Rapp CR, Curtis VF, Bayless A, Fletcher A, Glover LE, Evans CM, Jedlicka P, Furuta GT, de Zoeten EF, Colgan SP, and Eltzschig HK (2015) Epithelial-specific A2B adenosine receptor signaling protects the colonic epithelial barrier during acute colitis. *Mucosal Immunol* 8, 1324–1338 [PubMed: 25850656]
48. Paoliello-Paschoalato AB, Azzolini AE, Cruz MF, Marchi LF, Kabeya LM, Donadi EA, and Lucisano-Valim YM (2014) Isolation of healthy individuals' and rheumatoid arthritis patients' peripheral blood neutrophils by the gelatin and Ficoll-Hypaque methods: comparative efficiency and impact on the neutrophil oxidative metabolism and Fcγ receptor expression. *J Immunol Methods* 412, 70–77 [PubMed: 25017507]
49. Wang X, Spandidos A, Wang H, and Seed B (2012) PrimerBank: a PCR primer database for quantitative gene expression analysis, 2012 update. *Nucleic Acids Res* 40, D1144–1149 [PubMed: 22086960]
50. Assarsson E, Lundberg M, Holmquist G, Bjorkesten J, Thorsen SB, Ekman D, Eriksson A, Rennel Dickens E, Ohlsson S, Edfeldt G, Andersson AC, Lindstedt P, Stenvang J, Gullberg M, and Fredriksson S (2014) Homogenous 96-plex PEA immunoassay exhibiting high sensitivity, specificity, and excellent scalability. *PLoS One* 9, e95192 [PubMed: 24755770]
51. Mayer M, and Meyer B (1999) Characterization of Ligand Binding by Saturation Transfer Difference NMR Spectroscopy. *Angew Chem Int Ed Engl* 38, 1784–1788 [PubMed: 29711196]
52. Delaglio F, Grzesiek S, Vuister GW, Zhu G, Pfeifer J, and Bax A (1995) NMRPipe: a multidimensional spectral processing system based on UNIX pipes. *J Biomol NMR* 6, 277–293 [PubMed: 8520220]
53. Pinero-Fernandez S, Chimere C, Keyser UF, and Summers DK (2011) Indole transport across *Escherichia coli* membranes. *J Bacteriol* 193, 1793–1798 [PubMed: 21296966]
54. Bean RC, Shepherd WC, and Chan H (1968) Permeability of lipid bilayer membranes to organic solutes. *J Gen Physiol* 52, 495–508 [PubMed: 5673304]

55. DeChatelet LR, Shirley PS, and Johnston RB Jr. (1976) Effect of phorbol myristate acetate on the oxidative metabolism of human polymorphonuclear leukocytes. *Blood* 47, 545–554 [PubMed: 1260119]
56. Fligel SE, Lee EC, McCoy JP, Johnson KJ, and Varani J (1984) Protein degradation following treatment with hydrogen peroxide. *Am J Pathol* 115, 418–425 [PubMed: 6375392]
57. Wei Z, Bai O, Richardson JS, Mousseau DD, and Li XM (2003) Olanzapine protects PC12 cells from oxidative stress induced by hydrogen peroxide. *J Neurosci Res* 73, 364–368 [PubMed: 12868070]
58. Ilyasov IR, Beloborodov VL, Selivanova IA, and Terekhov RP (2020) ABTS/PP Decolorization Assay of Antioxidant Capacity Reaction Pathways. *Int J Mol Sci* 21
59. Mor M, Spadoni G, Diamantini G, Bedini A, Tarzia G, Silva C, Vacondio F, Rivara M, Plazzi PV, Franceschini D, Zusso M, and Giusti P (2003) Antioxidant and cytoprotective activity of indole derivatives related to melatonin. *Adv Exp Med Biol* 527, 567–575 [PubMed: 15206775]
60. Herraiz T, and Galisteo J (2004) Endogenous and dietary indoles: a class of antioxidants and radical scavengers in the ABTS assay. *Free Radic Res* 38, 323–331 [PubMed: 15129740]
61. Darkoh C, Plants-Paris K, Bishoff D, and DuPont HL (2019) Clostridium difficile Modulates the Gut Microbiota by Inducing the Production of Indole, an Interkingdom Signaling and Antimicrobial Molecule. *mSystems* 4
62. Darkoh C, Chappell C, Gonzales C, and Okhuysen P (2015) A rapid and specific method for the detection of indole in complex biological samples. *Appl Environ Microbiol* 81, 8093–8097 [PubMed: 26386049]
63. Wienken CJ, Baaske P, Rothbauer U, Braun D, and Duhr S (2010) Protein-binding assays in biological liquids using microscale thermophoresis. *Nat Commun* 1, 100 [PubMed: 20981028]
64. Venkitakrishnan RP, Benard O, Max M, Markley JL, and Assadi-Porter FM (2012) Use of NMR saturation transfer difference spectroscopy to study ligand binding to membrane proteins. *Methods Mol Biol* 914, 47–63 [PubMed: 22976022]
65. Haselhorst T, Lamerz AC, and Itzstein M (2009) Saturation transfer difference NMR spectroscopy as a technique to investigate protein-carbohydrate interactions in solution. *Methods Mol Biol* 534, 375–386 [PubMed: 19277538]
66. Kettle AJ, Gedye CA, Hampton MB, and Winterbourn CC (1995) Inhibition of myeloperoxidase by benzoic acid hydrazides. *Biochem J* 308 (Pt 2), 559–563 [PubMed: 7772042]
67. Kettle AJ, Gedye CA, and Winterbourn CC (1997) Mechanism of inactivation of myeloperoxidase by 4-aminobenzoic acid hydrazide. *Biochem J* 321 (Pt 2), 503–508 [PubMed: 9020887]
68. Rosales C, Demaurex N, Lowell CA, and Uribe-Querol E (2016) Neutrophils: Their Role in Innate and Adaptive Immunity. *J Immunol Res* 2016, 1469780 [PubMed: 27006954]
69. Phillipson M, and Kubes P (2019) The Healing Power of Neutrophils. *Trends Immunol* 40, 635–647 [PubMed: 31160208]
70. Wang J (2018) Neutrophils in tissue injury and repair. *Cell Tissue Res* 371, 531–539 [PubMed: 29383445]
71. Muthas D, Reznichenko A, Balendran CA, Bottcher G, Clausen IG, Karrman Mardh C, Ottosson T, Uddin M, MacDonald TT, Danese S, and Berner Hansen M (2017) Neutrophils in ulcerative colitis: a review of selected biomarkers and their potential therapeutic implications. *Scand J Gastroenterol* 52, 125–135 [PubMed: 27610713]
72. Boughton-Smith NK, Evans SM, Hawkey CJ, Cole AT, Balsitis M, Whittle BJ, and Moncada S (1993) Nitric oxide synthase activity in ulcerative colitis and Crohn's disease. *Lancet* 342, 338–340 [PubMed: 7687730]
73. Zuo T, and Ng SC (2018) The Gut Microbiota in the Pathogenesis and Therapeutics of Inflammatory Bowel Disease. *Front Microbiol* 9, 2247 [PubMed: 30319571]
74. Khan I, Ullah N, Zha L, Bai Y, Khan A, Zhao T, Che T, and Zhang C (2019) Alteration of Gut Microbiota in Inflammatory Bowel Disease (IBD): Cause or Consequence? IBD Treatment Targeting the Gut Microbiome. *Pathogens* 8
75. Ni J, Wu GD, Albenberg L, and Tomov VT (2017) Gut microbiota and IBD: causation or correlation? *Nat Rev Gastroenterol Hepatol* 14, 573–584 [PubMed: 28743984]

76. Levy M, Thaïss CA, and Elinav E (2016) Metabolites: messengers between the microbiota and the immune system. *Genes Dev* 30, 1589–1597 [PubMed: 27474437]
77. Kim CH (2018) Immune regulation by microbiome metabolites. *Immunology* 154, 220–229 [PubMed: 29569377]
78. Bansal T, Alaniz RC, Wood TK, and Jayaraman A (2010) The bacterial signal indole increases epithelial-cell tight-junction resistance and attenuates indicators of inflammation. *Proc Natl Acad Sci U S A* 107, 228–233 [PubMed: 19966295]
79. Cervantes-Barragan L, Chai JN, Tianero MD, Di Luccia B, Ahern PP, Merriman J, Cortez VS, Caparon MG, Donia MS, Gilfillan S, Cella M, Gordon JI, Hsieh CS, and Colonna M (2017) *Lactobacillus reuteri* induces gut intraepithelial CD4(+)CD8 α alpha(+) T cells. *Science* 357, 806–810 [PubMed: 28775213]
80. Roager HM, and Licht TR (2018) Microbial tryptophan catabolites in health and disease. *Nat Commun* 9, 3294 [PubMed: 30120222]
81. Krishnan S, Ding Y, Saedi N, Choi M, Sridharan GV, Sherr DH, Yarmush ML, Alaniz RC, Jayaraman A, and Lee K (2018) Gut Microbiota-Derived Tryptophan Metabolites Modulate Inflammatory Response in Hepatocytes and Macrophages. *Cell Rep* 23, 1099–1111 [PubMed: 29694888]
82. Arora AK, and Kamaluddin. (2011) Studies on the Characterization and Interaction of Indole with Fe₂O₃/Cr₂O₃ Using Spectroscopic Methods. *Adsorpt Sci Technol* 29, 39–46
83. Manchanda K, Kolarova H, Kerkenpass C, Mollenhauer M, Vitecek J, Rudolph V, Kubala L, Baldus S, Adam M, and Klinke A (2018) MPO (Myeloperoxidase) Reduces Endothelial Glycocalyx Thickness Dependent on Its Cationic Charge. *Arterioscler Thromb Vasc Biol* 38, 1859–1867 [PubMed: 29903730]
84. Churg A, Marshall CV, Sin DD, Bolton S, Zhou S, Thain K, Cadogan EB, Maltby J, Soars MG, Mallinder PR, and Wright JL (2012) Late intervention with a myeloperoxidase inhibitor stops progression of experimental chronic obstructive pulmonary disease. *Am J Respir Crit Care Med* 185, 34–43 [PubMed: 21997333]
85. Chai W, Aylor K, Liu Z, Gan LM, Michaelsson E, and Barrett E (2019) Inhibiting myeloperoxidase prevents onset and reverses established high-fat diet-induced microvascular insulin resistance. *Am J Physiol Endocrinol Metab* 317, E1063–E1069 [PubMed: 31593502]
86. Jucaite A, Svenningsson P, Rinne JO, Cselenyi Z, Varnas K, Johnstrom P, Amini N, Kirjavainen A, Helin S, Minkwitz M, Kugler AR, Posener JA, Budd S, Halldin C, Varrone A, and Farde L (2015) Effect of the myeloperoxidase inhibitor AZD3241 on microglia: a PET study in Parkinson's disease. *Brain* 138, 2687–2700 [PubMed: 26137956]
87. Vinolo MA, Rodrigues HG, Hatanaka E, Sato FT, Sampaio SC, and Curi R (2011) Suppressive effect of short-chain fatty acids on production of proinflammatory mediators by neutrophils. *J Nutr Biochem* 22, 849–855 [PubMed: 21167700]
88. Zhang D, and Frenette PS (2019) Cross talk between neutrophils and the microbiota. *Blood* 133, 2168–2177 [PubMed: 30898860]
89. Chen MX, Wang SY, Kuo CH, and Tsai IL (2019) Metabolome analysis for investigating host-gut microbiota interactions. *J Formos Med Assoc* 118 Suppl 1, S10–S22 [PubMed: 30269936]
90. Bendheim PE, Poeggeler B, Neria E, Ziv V, Pappolla MA, and Chain DG (2002) Development of indole-3-propionic acid (OXIGON) for Alzheimer's disease. *J Mol Neurosci* 19, 213–217 [PubMed: 12212784]
91. Hwang IK, Yoo KY, Li H, Park OK, Lee CH, Choi JH, Jeong YG, Lee YL, Kim YM, Kwon YG, and Won MH (2009) Indole-3-propionic acid attenuates neuronal damage and oxidative stress in the ischemic hippocampus. *J Neurosci Res* 87, 2126–2137 [PubMed: 19235887]
92. Chyan YJ, Poeggeler B, Omar RA, Chain DG, Frangione B, Ghiso J, and Pappolla MA (1999) Potent neuroprotective properties against the Alzheimer beta-amyloid by an endogenous melatonin-related indole structure, indole-3-propionic acid. *J Biol Chem* 274, 21937–21942 [PubMed: 10419516]
93. Yisireyli M, Takeshita K, Saito S, Murohara T, and Niwa T (2017) Indole-3-propionic acid suppresses indoxyl sulfate-induced expression of fibrotic and inflammatory genes in proximal tubular cells. *Nagoya J Med Sci* 79, 477–486 [PubMed: 29238104]

94. Ji Y, Gao Y, Chen H, Yin Y, and Zhang W (2019) Indole-3-Acetic Acid Alleviates Nonalcoholic Fatty Liver Disease in Mice via Attenuation of Hepatic Lipogenesis, and Oxidative and Inflammatory Stress. *Nutrients* 11
95. Ji Y, Yin W, Liang Y, Sun L, Yin Y, and Zhang W (2020) Anti-Inflammatory and Anti-Oxidative Activity of Indole-3-Acetic Acid Involves Induction of HO-1 and Neutralization of Free Radicals in RAW264.7 Cells. *Int J Mol Sci* 21
96. Kuenzig ME, Bishay K, Leigh R, Kaplan GG, Benchimol EI, and Crowdscreen SRRT (2018) Co-occurrence of Asthma and the Inflammatory Bowel Diseases: A Systematic Review and Meta-analysis. *Clin Transl Gastroenterol* 9, 188 [PubMed: 30250122]
97. Chen Y, Chen L, Xing C, Deng G, Zeng F, Xie T, Gu L, and Yang H (2020) The risk of rheumatoid arthritis among patients with inflammatory bowel disease: a systematic review and meta-analysis. *BMC Gastroenterol* 20, 192 [PubMed: 32552882]
98. Zhang N, Ju Z, and Zuo T (2018) Time for food: The impact of diet on gut microbiota and human health. *Nutrition* 51–52, 80–85
99. Shurney D, and Pauly K (2019) The Gut Microbiome and Food as Medicine: Healthy Microbiomes = Healthy Humans. *Am J Health Promot* 33, 821–824 [PubMed: 31120342]

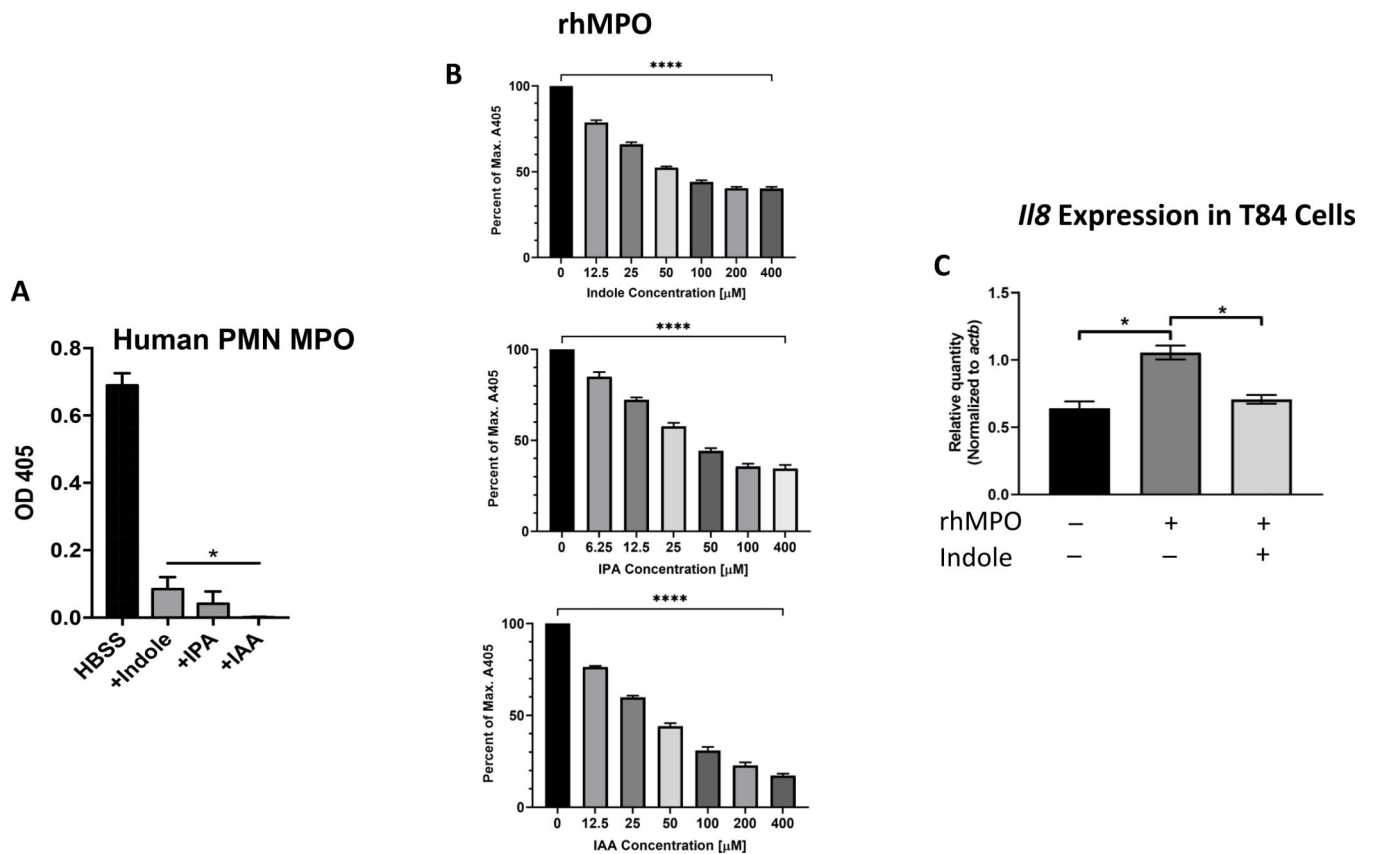


Figure 1. Indole metabolites inhibit neutrophil myeloperoxidase activity.

(A) Primary human PMN lysates were incubated with or without indole derivatives at 1 mM, and myeloperoxidase (MPO) activity was measured by ABTS assay at 405nm. (B) Recombinant human MPO (rhMPO) was incubated in the presence various indole metabolites at various doses and measured by ABTS. Data represented as percent of maximum absorbance at 405nm. All concentrations of indole compounds significantly reduced A405 by one-way ANOVA (**** $p < 0.0001$). (C) Expression of *i/8* in T84 cells was evaluated by qRT-PCR after treatment with either 10 $\mu\text{g/mL}$ rhMPO or rhMPO + 0.833 mM indole as described in the Materials & Methods section. Gene expression was normalized to *actb* and compared with untreated control cells. $p < 0.001$ using t test (two tailed, two sample heteroscedastic).

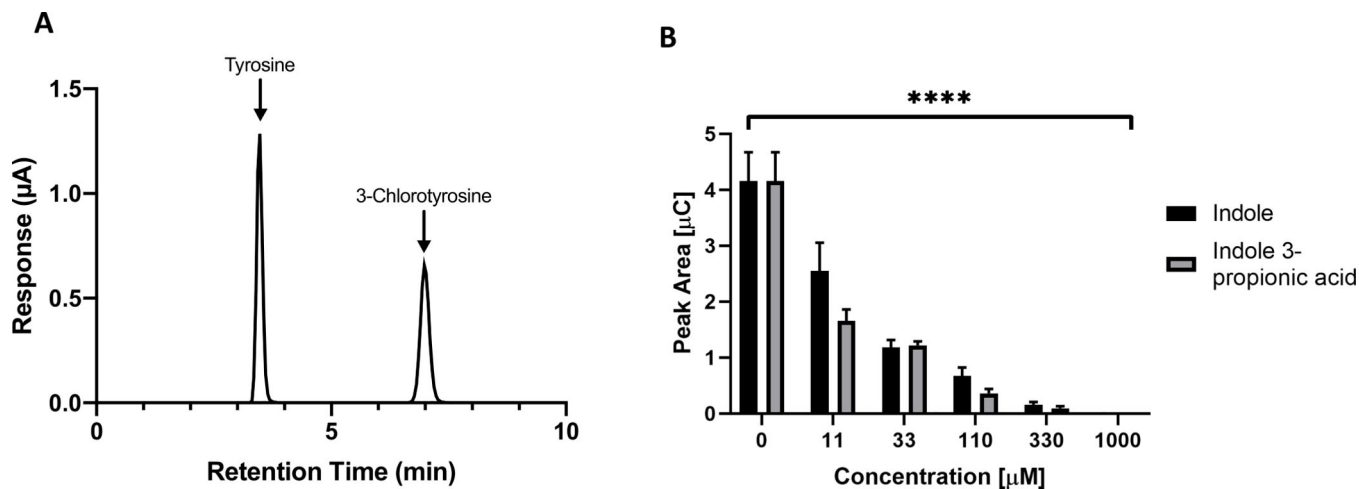


Figure 2. Indole and Indole 3-propionic acid (IPA) inhibit MPO-mediated tyrosine chlorination. (A) EC-HPLC tracing of tyrosine and 3-chlorotyrosine. (B) Recombinant MPO and H₂O₂ were reacted with free tyrosine in vitro and with varying concentrations of either indole or IPA. Chlorination of tyrosine was detected by EC-HPLC as demonstrated in Fig. 2A, with increased detection of 3-chlorotyrosine reflected in a greater detected peak area (y-axis). Decrease in peak area was significant for both indole and IPA at all concentrations tested. **** $p < 0.0001$ by one-way ANOVA.

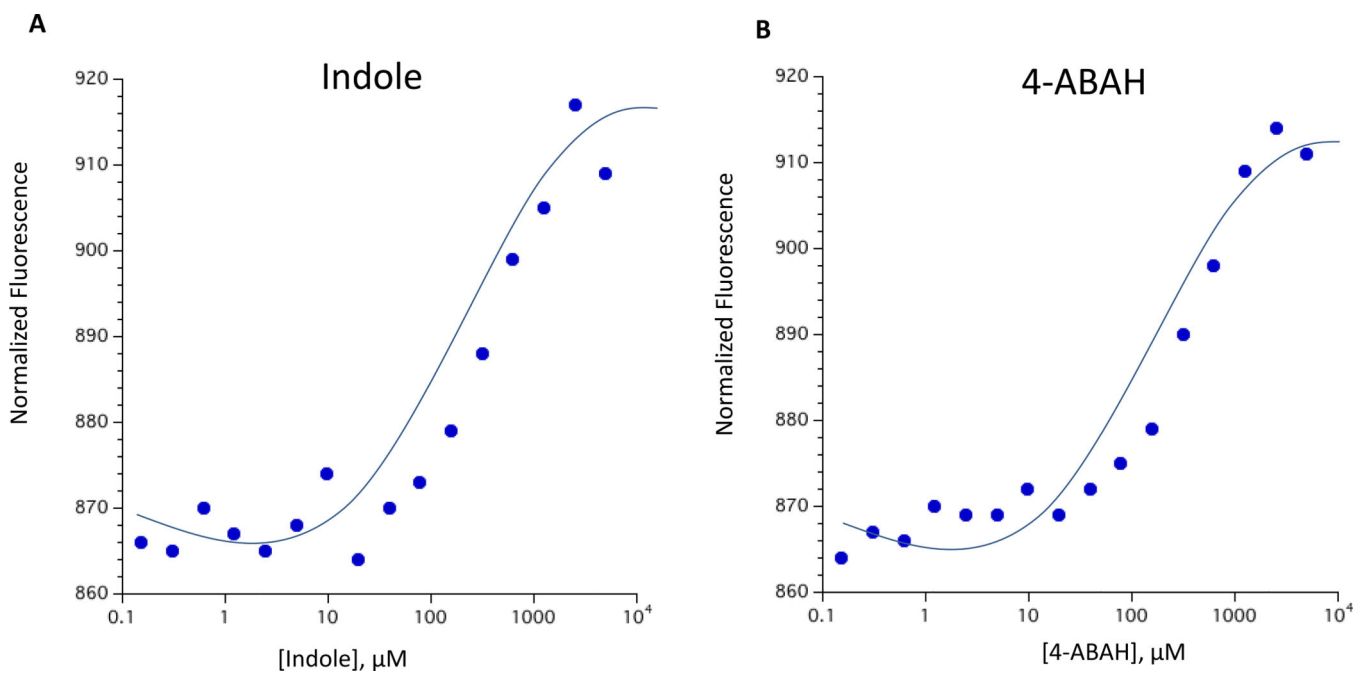


Figure 3. Indole interacts with and binds MPO by microscale thermophoresis (MST).

(A) Indole binds to rhMPO at a higher affinity compared to a commercially available MPO inhibitor, (B) 4-ABAH. MST assays yielded the indicated K_D values: Indole: 272 ± 77.4 μM ; 4-ABAH: 409 ± 66.7 μM . Sixteen serial dilutions of every ligand were mixed with fluorescently labeled his-tagged rhMPO in standard capillary tubes. (Data are presented as mean \pm SEM).

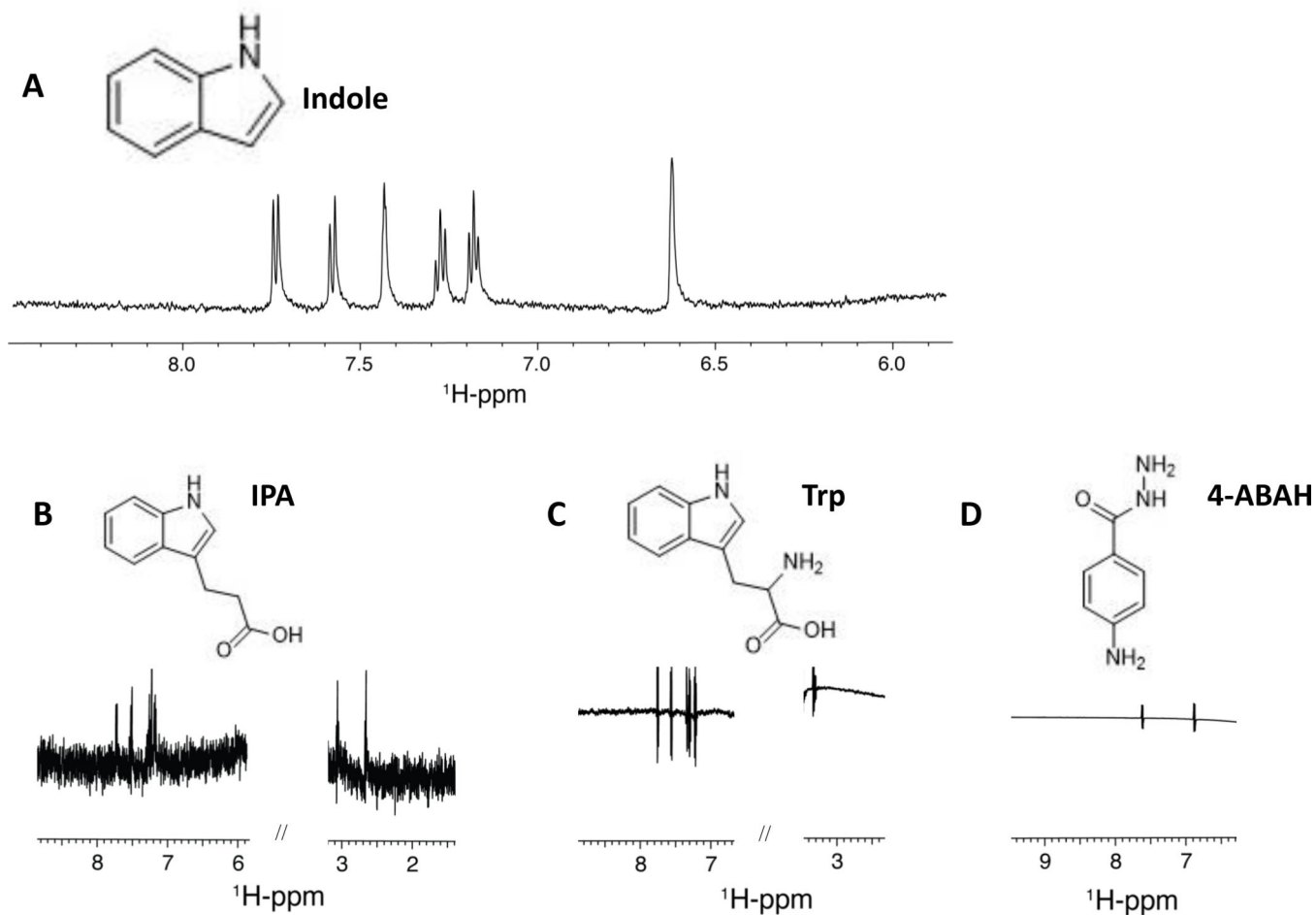


Figure 4. Indole metabolites exhibit ligand binding to myeloperoxidase by NMR Saturation Transfer Difference (STD).

1D ^1H -STD NMR spectra of $9\ \mu\text{M}$ rhMPO in association with $1\ \text{mM}$ aqueous solutions of the ligands (A) indole, (B) indole-3-propionic acid, (C) tryptophan, (D) 4-ABAH. The corresponding ligand structure is shown on top of each spectrum.

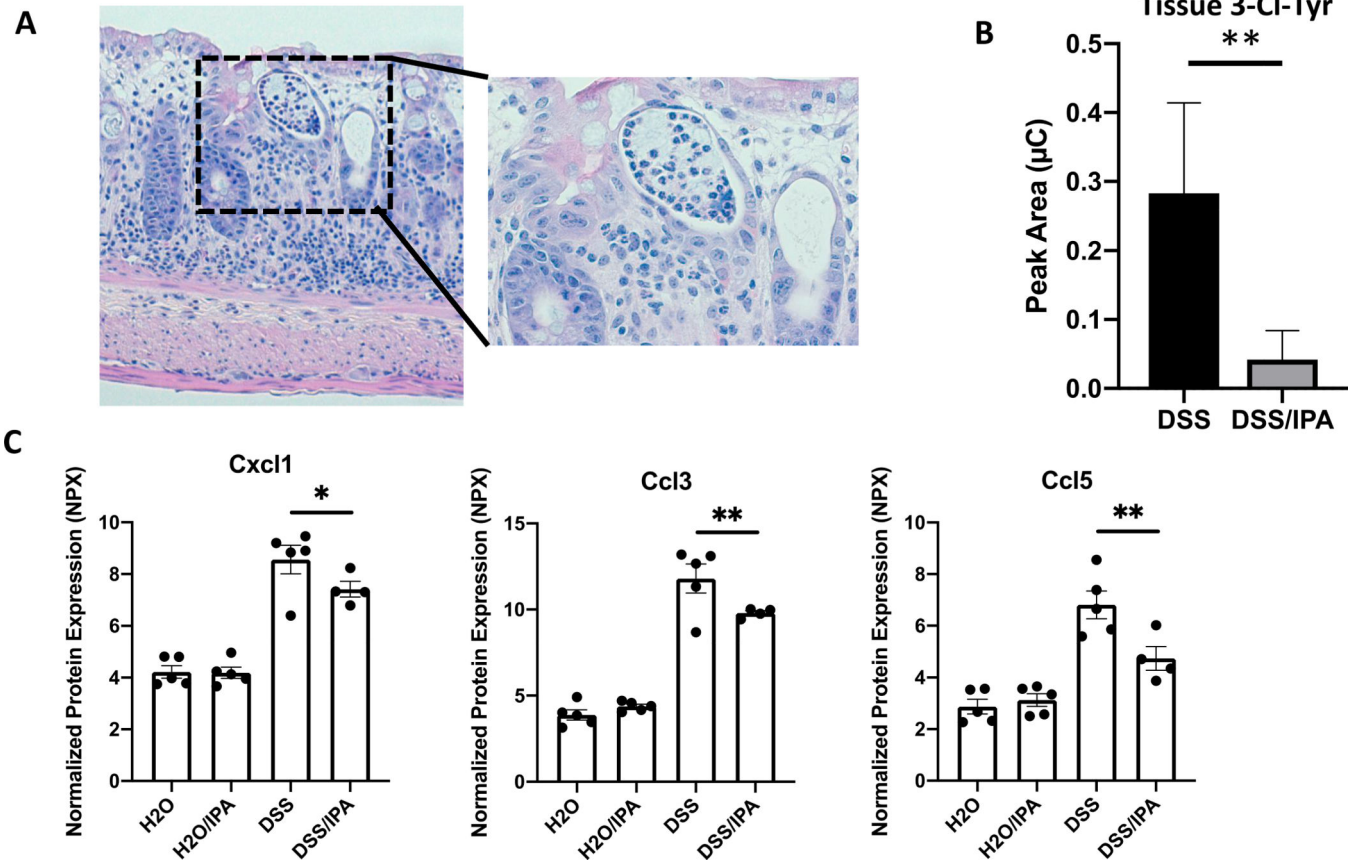


Figure 5. Indole-3-propionic acid (IPA) alters intestinal crypt abscess and chemokine expression in a dextran sodium sulfate (DSS) colitis model.

(A) Staining of colon tissue from DSS-treated mice reveals significant inflammation-associated alterations, including formation of large crypt abscesses (see inset); (B) Mouse colon samples were digested with Pronase overnight at 37 °C to yield free amino acids, and levels of chlorinated tyrosine (3-Cl-Tyr) in animals administered DSS were detected by EC-HPLC (N = 5 mice/group). (C) Tissue chemokine expression in mice with treated with/without DSS and with/without IPA was quantified using Olink proximity extension amplification. Results indicate that expression of pro-inflammatory chemokines is significantly increased in DSS colitis and decreased with the addition of IPA treatment. N = 4–5 mice per group.

Table 1:

qRT-PCR primers used in this study

Primer Name	Fwd Seq. (5'→3')	Rev Seq. (5'→3')	Source
Human <i>actb</i>	CATGTACGTTGCTATCCAGGC	CTCCTTAATGTCACGCACGAT	Harvard PrimerBank ID# 4501885a1
Human <i>il8 (cxcl8)</i>	TTTGCCAAGGAGTGCTAAAGA	AACCCTCTGCACCCAGTTTTC	Harvard PrimerBank ID# 10834978a1

Author Manuscript

Author Manuscript

Author Manuscript

Author Manuscript